Communications in Computational Chemistry
Commun. Comput. Chem., Vol. 7, No. 4, 325–330
doi: 10.4208/cicc.2025.212.01
Regular Article

Computational Study on the Reaction Mechanism of LigW-Catalyzed Carboxylation of Monohydroxybenzoic Acids

Qinrou Li[1,2], Shiqing Zhang[1], Wei Wang[1,3], Hao Su[1,3] and Xiang Sheng[1,3,*]

[1]*State Key Laboratory of Engineering Biology for Low-Carbon Manufacturing, Tianjin Institute of Industrial Biotechnology, Chinese Academy of Sciences, Tianjin 300308, P. R. China;*

[2]*Haihe Laboratory of Synthetic Biology, Tianjin 300308, P. R. China;*

[3]*National Center of Technology Innovation for Synthetic Biology and National Engineering Research Center of Industrial Enzymes, Tianjin 300308, P. R. China.*

[*] Corresponding author: shengx@tib.cas.cn

Received on 31 July 2025; Accepted on 8 August 2025

Abstract: Enzymatic carboxylation of phenols via the Kolbe-Schmitt reaction represents a promising sustainable strategy for CO_2 fixation and synthesis of high-value chemicals. This study investigates the reaction mechanism of 5-carboxyvanillate decarboxylase (LigW)-catalyzed carboxylation of non-natural monohydroxybenzoic acids, employing the quantum chemical cluster approach. First, we investigate the carboxylation mechanism of 4-hydroxybenzoate (4-HBA) to produce 4-hydroxyisophthalate (4-HIPA), a dicarboxylic acid with potent antioxidant and neuroprotective applications. The calculations reveal that the CO_2-binding mediates the preferred binding mode of the substrates and the incorporation of CO_2 to the active site favors the mode beneficial for the following reaction. The chemical reaction is initiated by the formation of a carbon-carbon bond between CO_2 and 4-HBA, followed by the rate-limiting proton transfer from the active site residue Asp314 to the resulting intermediate of the first step with a calculated barrier of 19.2 kcal/mol. Additionally, the potential of LigW in catalyzing the carboxylation of 3-hydroxybenzoate (3-HBA) is evaluated, and the calculations show that the reaction is energetically unfeasible due to the prohibitively high barrier of chemical steps. These mechanistic insights, together with the previous studies on the natural substrate, provide important information for the rotational design of LigW variants for industrial biocatalysis and CO_2 utilization.

Key words: carboxylation, reaction mechanism, quantum chemical cluster approach, biocatalysis, decarboxylase.

1. Introduction

As environmental challenges such as rising carbon dioxide (CO_2) levels intensify, developing efficient CO_2 fixation strategies has become critical. Enzymatic approaches, particularly those utilizing carboxylating enzymes, offer a promising avenue for converting CO_2 into valuable chemical products [1-3]. 5-Carboxyvanillate decarboxylase (LigW), an enzyme playing a key role in microbial lignin degradation, holds significant potential as a biotechnological tool for carbon utilization as it has been established to display carboxylation activity, in addition to its natural decarboxylation activity [4].

The reaction catalyzed by LigW in nature, the decarboxylation of 5-carboxyvanillate (Scheme 1a), has been studied using computational and experimental approaches [5-7]. It was proposed that the decarboxylation reaction proceeds through a two-step mechanism, requiring the formation of a C5-protonated intermediate before the carbon-carbon bond cleavage and the subsequent formation of the product and CO_2.

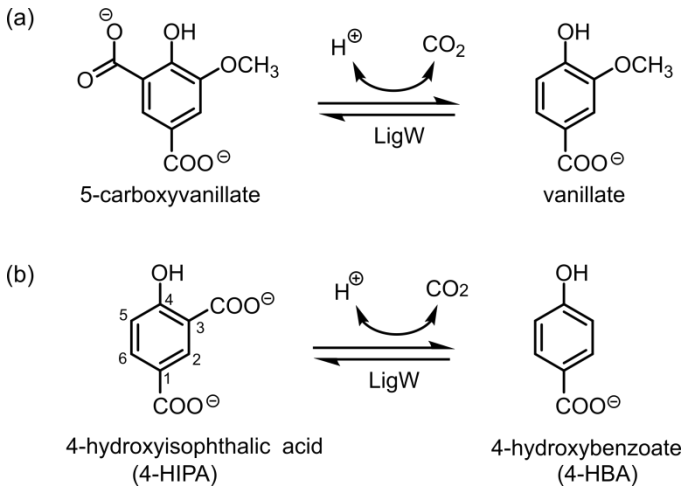

Scheme 1. LigW-catalyzed interconversion (a) between 5-carboxyvanillate and vanillate and (b) between 4-hydroxyisophthalate (4-HIPA) and 4-hydroxybenzoate (4-HBA).

A recent study demonstrated the use of LigW in catalyzing the carboxylation reaction of 4-hydroxybenzoate (4-HBA) to synthesize 4-hydroxyisophthalate (4-HIPA) (Scheme 1b), laying the groundwork for its biocatalytic application in CO_2 fixation [8]. The bio-carboxylation of aromatic and phenolic compounds is an environmental-friendly method for producing high-value aromatic carboxylic acids, in particular the dicarboxylic acid, which has been recognized for its potential application as a novel cell-protective antioxidant [9,10]. A number of other decarboxylases from the same family as LigW, namely the amidohydrolase superfamily, have also been proven to display carboxylation activities on aromatic and phenolic compounds [1-3,11]. These reactions align with the mechanistic principles of the traditional chemical Kolbe–Schmitt reaction, adapted thus as the Bio-Kolbe-Schmitt reaction in biological systems. Despite extensive studies having been performed on these enzymes [1-3,11,12], the mechanism of the LigW-catalyzed carboxylation of the non-natural monohydroxybenzoate 4-HBA remains unsolved, and the critical transition states and intermediates in the reaction and key amino acid residues regulating its activity are yet to be identified.

Detailed understanding of the reaction mechanism of LigW, especially the factors controlling its activity toward different substrates, is critical for optimizing its use in biocatalysis applications. In the present study, using the quantum chemical cluster approach, which is a powerful computational method for modeling enzymatic reactions [6,12-16], the mechanisms of the LigW-catalyzed carboxylation of monohydroxybenzoic acids are investigated. First, the binding mode of 4-HBA and the reaction pathway for its carboxylation are identified, and the corresponding energy profile is obtained. Subsequently, the feasibility of 3-hydroxybenzoate (3-HBA), a compound structurally similar to 4-HBA, was evaluated to probe the catalytic versatility and substrate selectivity of LigW. The computational insights provide a theoretical foundation for enhancing the applications of LigW in industrial biocatalysis.

2. Computational methods

2.1 Technical details

The B3LYP hybrid density functional method [17,18], incorporating D3 (BJ) dispersion corrections [19,20], was applied to all calculations presented in this study, as implemented in the Gaussian 16 program [21]. Geometry optimization was performed with 6-31g (d,p) basic sets for C, N, O, and H and LANL2DZ pseudopotential [22] for Mn. At the same level of theory as the geometry optimization, single-point energies were calculated using the SMD solvation model with $\varepsilon = 4$ [23]. Single-point calculations on the optimized structures were performed with LANL2DZ for Mn and the larger basis set 6-311+G (2d,2p) for the other atoms, ensuring improved accuracy in the energies. The zero-point energies (ZPEs) were calculated at the same level of geometry optimization. All reported values of the energies presented in the current study are the large basis set energies, corrected for ZPEs and solvation effects. The entropy contribution from binding or releasing a small gas molecule in the computational model was estimated by the translational entropy of the unbound molecule, following the previous studies [6,24-28]. The entropy of CO_2, calculated as 11.1 kcal/mol at room temperature, was incorporated into the energy of enzyme-CO_2 adduct formation. For the spin state of Mn^{2+}, the high-spin sextet state in the enzyme-substrate complex is energetically much favored over the low-spin doublet and quartet states by more than 30 kcal/mol. This trend is consistent with that reported in the previous computational study on the LigW-catalyzed reaction of the natural substrate [7]. Therefore, only the sextet state was considered for Mn^{2+} in the mechanistic study.

2.2 Model setup

Following the previous computational study on the LigW-catalyzed decarboxylation of the natural substrate [6], a large cluster model of the active site is here designed. The model was constructed on the basis of the high-resolution crystal structure of LigW from *Novosphingobium aromaticivorans*, with 5-nitrovanillate (5-NV) bound to the active site (PDB ID: 4QRN) [5]. In the current study, 5-NV was manually replaced by either 4-hydroxybenzoate (4-HBA) or 3-hydroxybenzoate (3-HBA) as substrates. In addition to the substrate, the model includes the Mn^{2+} cation and its coordinating ligands (Glu19, His188, Asp314, and Wat1), and the amino acids forming the active site (Leu47, Tyr51, Arg58, Thr90, Ser91, Tyr186, Gly207, Ala208, Ile209, Phe212, Val239, Gly240, His241, Glu244, Arg252, Arg265, Ser289, and Tyr317). Nine additional crystallographic water molecules were also incorporated. For both substrates, the hydroxyl and carboxyl groups of 4-HBA and 3-HBA are assumed to deprotonate upon binding to the active site, due to the coordination to Mn^{2+} or the hydrogen bond interactions with Tyr51 and Arg265. Amino acids were truncated as shown in the corresponding figures, and hydrogen atoms were added manually to saturate the truncated atoms. To prevent unrealistic movements during geometry optimizations, certain atoms were constrained to their crystallographic positions, as specified in Figure S1. Both 4-HBA and 3-HBA models comprise 301 atoms and have a total charge of +1.

3. Results and discussion

3.1 Reaction mechanism of 4-HBA carboxylation

By analyzing the active site structure, it can be envisioned that 4-HBA binds via either phenolate-metal coordination or carboxylate-metal coordination, with the uncoordinated group engaging Tyr51 and Arg265 through hydrogen bonds. We first optimized the model with 4-HBA bound but not CO_2 (Figure 1a). It was shown that the mode with the carboxylate-metal coordination (**E:4-HBA'**) is more stable than the phenolate-metal coordination (**E:4-HBA**), with a calculated energy difference of 1.1 kcal/mol. This stability difference originates from enhanced hydrogen bonding in the carboxylate-bound mode. Specifically, two hydrogen bonds are formed between the substrate and residues (Tyr51 and Arg265) in both modes, but two additional hydrogen bonds are formed with surrounding water molecules in **E:4-HBA'**, compared to only one in **E:4-HBA**.

However, upon the introduction of CO_2, the trend of the stability of two binding modes is inverted. In the enzyme-substrate-CO_2 complex (Figure 1b), the phenolate-metal coordination (**E:4-HBA:CO_2**) becomes more favorable, with an energy of 2.9 kcal/mol lower than the carboxylate-metal coordination (**E:4-HBA:CO_2'**). Structural analysis reveals that the former accommodates the CO_2 molecule by forming a better hydrogen bond network and also the interaction with the Mn^{2+}. On the basis of these results, **E:4HBA:CO_2** is identified as the more plausible starting point for the carboxylation reaction. However, since the energy difference between the two modes is small, both modes are considered for the following mechanistic study.

The calculations show that the reaction pathway starting from **E:4HBA:CO_2** is energetically feasible (discussed below), while the pathway starting from **E:4HBA:CO_2'** is kinetically inaccessible with the energy of the intermediate exceeding 50 kcal/mol according to a scan of the energy along the C-C bond formation between the C3 atom of 4-HBA and the C atom of CO_2 (Figure S2). The prohibitively high energy in the latter case can be attributed to this specific orientation of the substrate where the newly-formed carboxylate group of the intermediate cannot form a beneficial coordination bond with the active site Mn^{2+} cation.

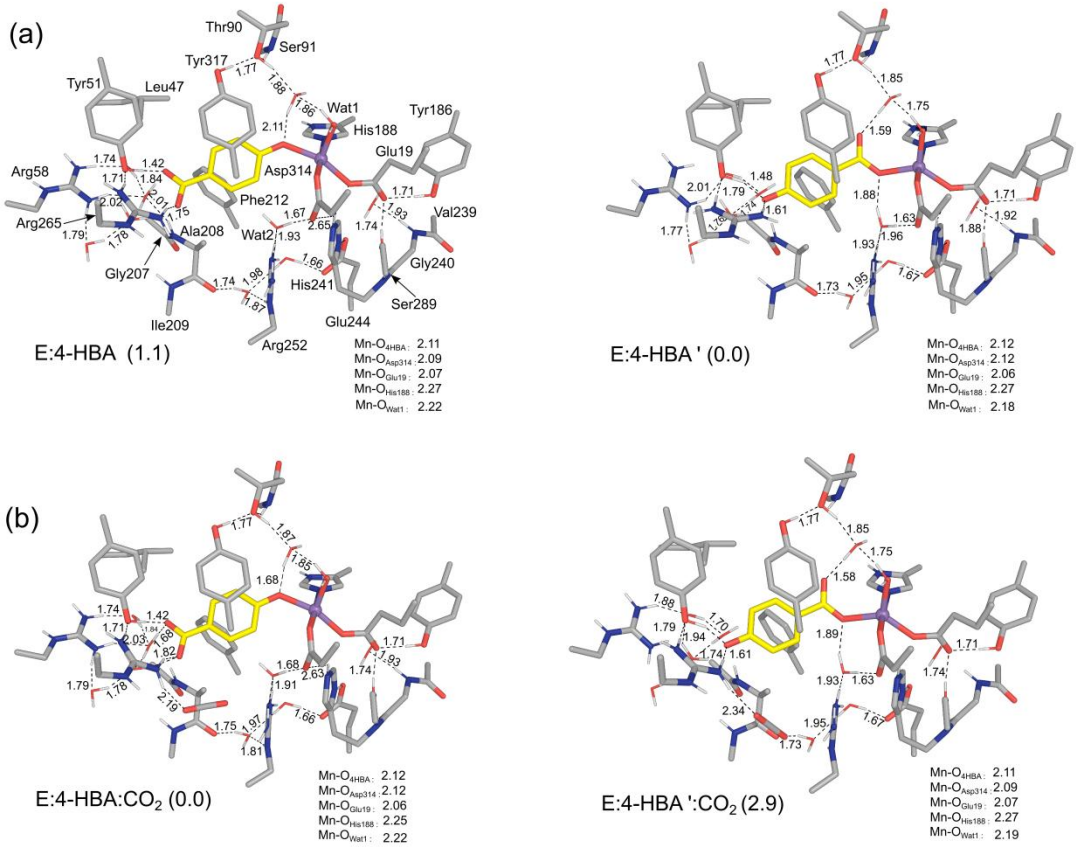

Figure 1. Two considered binding modes of 4-HBA for the carboxylation reaction catalyzed by LigW. (a) Complexes with 4-HBA bound but not CO_2, and (b) ternary complexes with both 4-HBA and CO_2 bound. Relative energies (in kcal/mol) are referenced to the more stable conformation in each panel. Selected distances are shown in Å.

The proposed mechanism of LigW-catalyzed carboxylation of 4-HBA and the corresponding energy profile are shown in Figure 2a and 2b, respectively. The optimized geometries of all transition states and intermediates are illustrated in Figure 2c. The CO_2 binding process is associated with an energy penalty of 5.4 kcal/mol (**E:4-HBA'** to **E:4-HBA:CO_2**), including the entropy contribution. Following CO_2 binding, the catalytic cycle proceeds via a two-step mechanism. The first step involves nucleophilic attack by the C3 carbon of the 4-HBA phenyl ring on CO_2, forming a carboxyvanillate intermediate (**Int1**) via the transition state **TS1**.

The calculated energy barrier for this C-C bond formation is 16.8 kcal/mol, relative to **E:4-HBA'**. Structural analysis of **TS1** reveals significant conformational changes on the substrate (Figure 2), mainly including the tetrahedral rehybridization at the attacking C3 center and the formation of carboxylate-Mn^{2+} coordination that expands the coordination number of Mn^{2+} from five to six. This direct coordination to the metal ion and the newly-formed hydrogen bond between the forming carboxylate group and Arg252 contribute to the stabilization of **TS1**.

The second step of the mechanism is the rearomatization of the phenyl ring via a proton transfer from the C3 carbon of the intermediate to Asp314 (Figure 2a), generating the final product, 4-hydroxyisophthalate (4-HIPA). This proton transfer process represents the rate-limiting step of the overall reaction, with a calculated energy barrier of 19.2 kcal/mol relative to the initial **E:4-HBA'** complex (Figure 2b). At the corresponding transition state (**TS2**, Figure 2c), the breaking C-H bond and the forming O-H bond are 1.34 Å and 1.35 Å, respectively. A key feature of **TS2** is the strengthening of the hydrogen bond between His241 and the Mn^{2+}-coordinated carboxylate group of the substrate, which shortens from 1.92 Å in **Int1** to 1.83 Å in **TS2**. The final **E:4-HIPA** complex is only 0.9 kcal/mol higher in energy than that of **E:4-HBA'**. In **E:4-HIPA**, the coordination bonds between Mn^{2+} and both the phenolic and carboxylate oxygen of the product are significantly shortened compared to that in **Int1**.

In summary, computational results demonstrate that CO_2 binding modulates the preferred binding mode of the 4-HBA substrate in the active site. In the absence of CO_2, the substrate prefers to bind in a non-productive binding mode, whereas CO_2 binding leads to the productive mode more favorable. For the chemical steps, we propose a mechanism for the LigW-catalyzed Bio-Kolbe-Schmitt reaction involving the C-C bond formation between the substrate and CO_2 and the following proton transfer from the intermediate to Asp314. The proton transfer represents the rate-limiting step with a calculated barrier of 19.2 kcal/mol, which is in excellent agreement with the experimental value of ca 20 kcal/mol converted from the measured k_{cat} of 0.00776 s^{-1} [8]. Notably, the barrier of 4-HBA carboxylation here is 2.4 kcal/mol higher than the activation barrier reported for the LigW natural reaction[6], consistent with experimental observation of lower carboxylation activities [6,8].

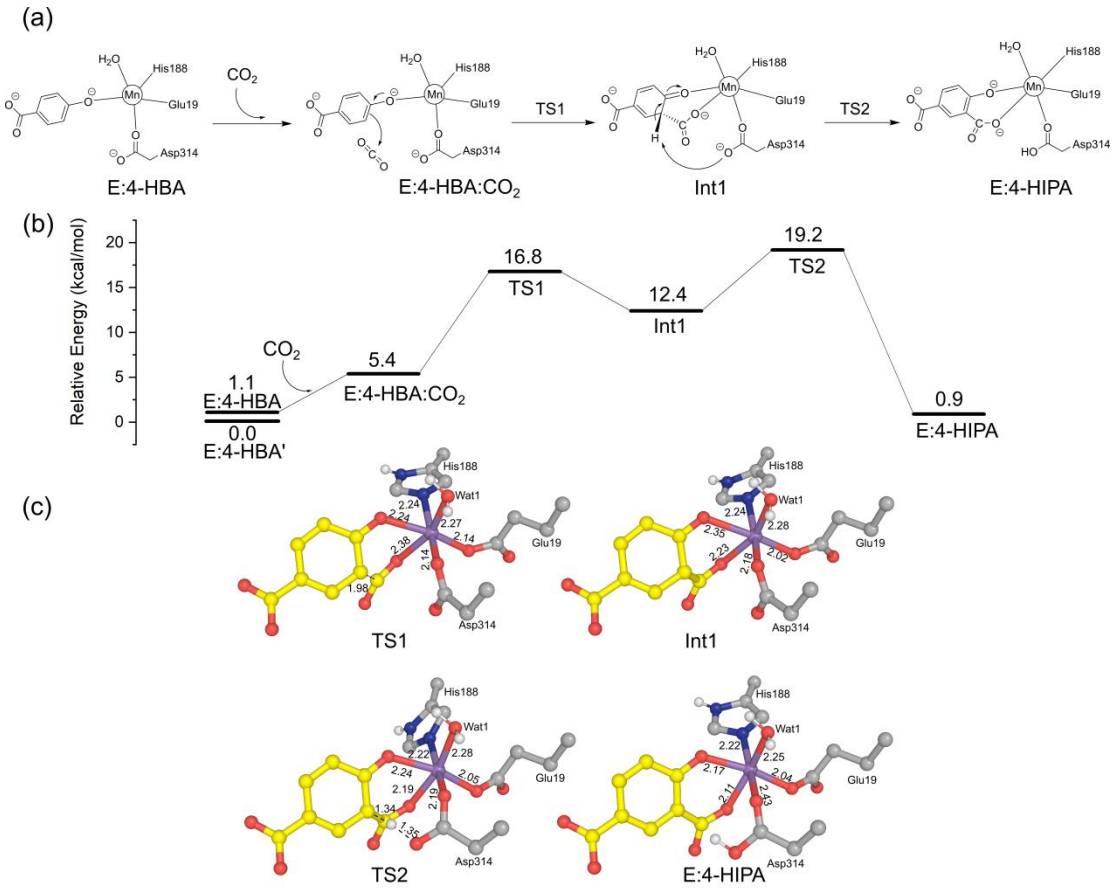

Figure 2. (a) Reaction mechanism of 4-HBA carboxylation catalyzed by LigW, (b) calculated energy profile, and (c) optimized structures of the stationary points along the proposed reaction pathway. Note that only a small part of the model is displayed here. See Figure S3 for the structures with the full model. Selected distances are shown in Å.

3.2 Evaluation of the catalytic feasibility of 3-HBA

Inspired by the catalytic capability of LigW in catalyzing the carboxylation of 4-HBA, we here use the quantum chemical calculations to evaluate its feasibility in carboxylating other monohydroxybenzates, choosing 3-hydroxybenzate (3-HBA) as a

representative substrate. Four binding modes of 3-HBA are considered, for which the optimized structures and corresponding energies are shown in Figure S4. It can be seen that in the lowest-energy binding mode, the phenolate group is coordinated to Mn^{2+} and the carboxylate group on the other site forms hydrogen bonds with Tyr51 and Arg58. The other binding modes of 3-HBA have much higher energies (> 8 kcal/mol). Therefore, only the lowest-energy mode is considered for the following mechanistic study.

Energy comparison of the enzyme-substrate complexes shows **E:3-HBA** is 0.3 kcal/mol more stable than **E:4-HBA'**, demonstrating their comparable binding affinities to the enzyme. The calculations on the chemical steps show that the CO_2 binding to the **E:3-HBA** is associated with an increase of the energy of 3.9 kcal/mol (**E:3-HBA** to **E:3-HBA:CO$_2$**, Figure 3), which is 1.5 kcal/mol lower than that in the case of 4-HBA. However, the calculated barrier of the overall reaction is 38.4 kcal/mol (see Figure S5 for the optimized structures and calculated energy profile), which is too high for an enzymatic reaction. According to these results, it can be concluded that LigW is very likely incapable of catalyzing the carboxylation of 3-HBA.

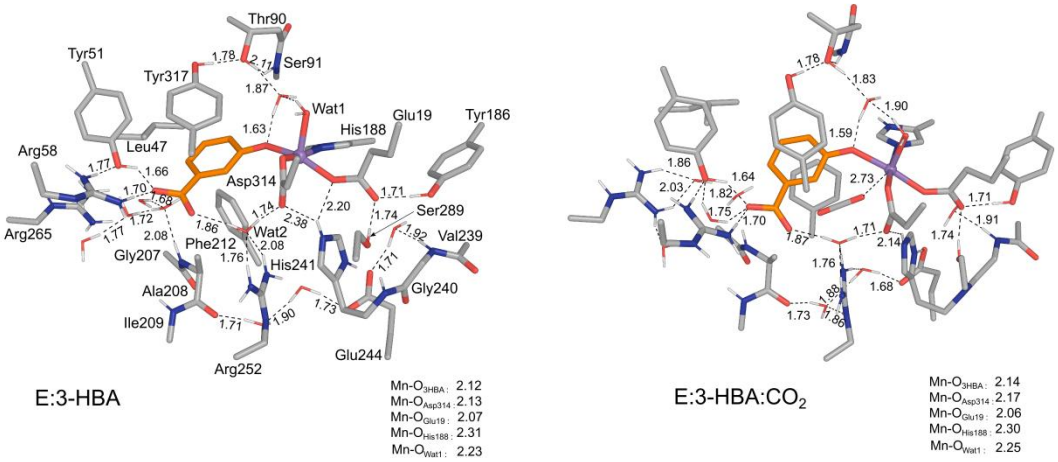

Figure 3. Optimized structures of the complexes with 3-HBA but not CO_2 bound **(E:3-HBA)**, and the ternary complexes with both 3-HBA and CO_2 bound (**E:3-HBA:CO$_2$**). Selected distances are shown in Å.

4. Conclusions

This study elucidates the complete catalytic mechanism of LigW-catalyzed Bio-Kolbe-Schmitt reaction, providing important insights into its unnatural carboxylation activity. Quantum chemical calculations demonstrate that CO_2 binding reposition 4-hydroxybenzoate (4-HBA) from a non-productive pose to a catalytically active mode that facilitates C-C bond formation. For the chemical steps, the carboxylation of 4-HBA is proposed to proceed via a two-step pathway, involving the C-C bond formation between the substrate and CO_2 and the following rate-limiting proton transfer from the intermediate to Asp314. The calculated overall barrier of the carboxylation reaction is 19.2 kcal/mol, which is in excellent agreement with the experimentally measured value. Current calculations also reveal that 3-hydroxybenzoate (3-HBA), a compound structurally similar to 4-HBA, cannot be carboxylated by LigW due to the prohibitively high activation barrier of the chemical steps. The mechanistic insights on the carboxylation activity of LigW in the present study provide important information to guide future protein engineering. For example, enhanced catalytic activity could be achieved by optimizing substrate binding modes and mutating second-shell residues to better stabilize the proton transfer transition state.

Supporting information

Optimized structures involved in the LigW-catalyzed carboxylation of 4-HBA; detailed results of the examined reaction of 3-HBA; calculated absolute energies; Cartesian coordinates. Additional information is available on this website: https://global-sci.com/storage/self-storage/cicc-2025-212-1-r1-si.pdf

Acknowledgments

This work was supported by the CAS Project for Young Scientists in Basic Research (No. YSBR-072-1), the Innovation Fund of Haihe Laboratory of Synthetic Biology (No. 22HHSWSS00020) and the Tianjin Synthetic Biotechnology Innovation Capacity Improvement Project (No. TSBICIP-CXRC-071).

Author contribution

X.S. conceived and supervised the research project. Q.L. performed the majority of computational work and data analysis. S.Z., W.W. and H.S. contributed to supplementary computational work, data analysis and scientific discussions. Q.L. drafted the initial manuscript, which was subsequently revised by X.S. with input from all co-authors.

Conflict of interest

The authors declare no competing financial interests.

References

[1] Payer S. E., Faber K. and Glueck S. M., Non-oxidative enzymatic (de)carboxylation of (hetero)aromatics and acrylic

acid derivatives. *Adv. Synth. Catal.*, **361** (11) (2019), 2402-2420.

[2] Bierbaumer S., Nattermann M., Schulz L., Zschoche R., Erb T. J., Winkler C. K., Tinzl M. and Glueck S. M., Enzymatic conversion of CO_2: From natural to artificial utilization. *Chem. Rev.*, **123** (9) (2023), 5702-5754.

[3] Liu B., Lin B., Su H. and Sheng X., Quantum chemical studies of the reaction mechanisms of enzymatic CO_2 conversion. *Phys. Chem. Chem. Phys.*, **26** (42) (2024), 26677-26692.

[4] Seibert C. M. and Raushel F. M., Structural and catalytic diversity within the amidohydrolase superfamily. *Biochemistry*, **44** (17) (2005), 6383-6391.

[5] Vladimirova A., Patskovsky Y., Fedorov A. A., Bonanno J. B., Fedorov E. V., Toro R., Hillerich B., Seidel R. D., Richards N. G. J. and Almo S. C., et al., Substrate distortion and the catalytic reaction mechanism of 5-carboxyvanillate decarboxylase. *J. Am. Chem. Soc.*, **138** (3) (2016), 826-836.

[6] Sheng X., Zhu W., Huddleston J., Xiang D. F., Raushel F. M., Richards N. G. J. and Himo F., A combined experimental-theoretical study of the LigW-catalyzed decarboxylation of 5-carboxyvanillate in the metabolic pathway for lignin degradation. *ACS Catal.*, **7** (8) (2017), 4968-4974.

[7] Prejanò M., Marino T. and Russo N., QM cluster or QM/MM in computational enzymology: The test case of LigW-decarboxylase. *Front. Chem.*, **6** (2018), 249.

[8] Zhang S., Zheng R., Long J., Zhu Y. and Tan T., Computational design of carboxylase for the synthesis of 4-hydroxyisophthalic acid from p-hydroxybenzoic acid by fixing CO_2. *J. Environ. Manage.*, **366** (2024), 121703.

[9] Haddadi M., Jahromi S. R., Nongthomba U., Shivanandappa T. and Ramesh S. R., 4-hydroxyisophthalic acid from Decalepis hamiltonii rescues the neurobehavioral deficit in transgenic Drosophila model of tauopathies. *Neurochem. Int.*, **100** (2016), 78-90.

[10] Niveditha S. and Shivanandappa T., Neuroprotective action of 4-hydroxyisophthalic acid against paraquat-induced motor impairment involves amelioration of mitochondrial damage and neurodegeneration in Drosophila. *Neurotoxicology*, **66** (2018), 160-169.

[11] Tommasi I. C., Carboxylation of hydroxyaromatic compounds with HCO_3^- by enzyme catalysis: Recent advances open the perspective for valorization of lignin-derived aromatics. *Catalysts*, **9** (1) (2019), 37.

[12] Sheng X. and Himo F., Mechanisms of metal-dependent non-redox decarboxylases from quantum chemical calculations. *Comput. Struct. Biotechnol. J.*, **19** (2021), 3176-3186.

[13] Sheng X., Kazemi M., Planas F. and Himo F., Modeling enzymatic enantioselectivity using quantum chemical methodology. *ACS Catal.*, **10** (11) (2020), 6430-6449.

[14] Siegbahn P. E. M., A quantum chemical approach for the mechanisms of redox-active metalloenzymes. *RSC Adv.*, **11** (6) (2021), 3495-3508.

[15] Sheng X. and Himo F., The quantum chemical cluster approach in biocatalysis. *Acc. Chem. Res.*, **56** (8) (2023), 938-947.

[16] de Visser S. P., Wong H. P. H., Zhang Y., Yadav R. and Sastri C. V., Tutorial review on the set-up and running of quantum mechanical models for enzymatic reaction mechanisms. *Chem. - Eur. J.*, **30** (60) (2024), e202402468.

[17] Lee C., Yang W. and Parr R. G., Development of the Colle-Salvetti correlation-energy formula into a functional of the electron density. *Phys. Rev. B*, **37** (2) (1988), 785-789.

[18] Becke A. D., Density-functional thermochemistry. III. The role of exact exchange. *J. Chem. Phys.*, **98** (7) (1993), 5648-5652.

[19] Grimme S., Antony J., Ehrlich S. and Krieg H., A consistent and accurate ab initio parametrization of density functional dispersion correction (DFT-D) for the 94 elements H-Pu. *J. Chem. Phys.*, **132** (15) (2010), 154104.

[20] Grimme S., Density functional theory with London dispersion corrections. *WIRes Comput. Mol. Sci.*, **1** (2) (2011), 211-228.

[21] Frisch M. J., Trucks G. W., Schlegel H. B., Scuseria G. E., Robb M. A., Cheeseman J. R., Scalmani G., Barone V., Petersson G. A., Nakatsuji H., Li X., Caricato M., Marenich A. V., Bloino J., Janesko B. G., Gomperts R., Mennucci B., Hratchian H. P., Ortiz J. V., Izmaylov A. F., Sonnenberg J. L., Williams-Young D., Ding F., Lipparini F., Egidi F., Goings J., Peng B., Petrone A., Henderson T., Ranasinghe D., Zakrzewski V. G., Gao J., Rega N., Zheng G., Liang W., Hada M., Ehara M., Toyota K., Fukuda R., Hasegawa J., Ishida M., Nakajima T., Honda Y., Kitao O., Nakai H., Vreven T., Throssell K., Montgomery J. A., Jr., Peralta J. E., Ogliaro F., Bearpark M. J., Heyd J. J., Brothers E. N., Kudin K. N., Staroverov V. N., Keith T. A., Kobayashi R., Normand J., Raghavachari K., Rendell A. P., Burant J. C., Iyengar S. S., Tomasi J., Cossi M., Millam J. M., Klene M., Adamo C., Cammi R., Ochterski J. W., Martin R. L., Morokuma K., Farkas O., Foresman J. B. and Fox D. J., Gaussian 16, Gaussian, Inc., Wallingford CT, 2019.

[22] Hay P. J. and Wadt W. R., Ab initio effective core potentials for molecular calculations. Potentials for the transition metal atoms Sc to Hg. *J. Chem. Phys.*, **82** (1) (1985), 270-283.

[23] Marenich A. V., Cramer C. J. and Truhlar D. G., Universal solvation model based on solute electron density and on a continuum model of the solvent defined by the bulk dielectric constant and atomic surface tensions. *J. Phys. Chem. B*, **113** (18) (2009), 6378-6396.

[24] Blomberg M. R. A. and Siegbahn P. E. M., Mechanism for N_2O generation in bacterial nitric oxide reductase: A quantum chemical study. *Biochemistry*, **51** (25) (2012), 5173-5186.

[25] Sheng X., Lind M. E. S. and Himo F., Theoretical study of the reaction mechanism of phenolic acid decarboxylase. *FEBS J.*, **282** (24) (2015), 4703-4713.

[26] Sheng X., Plasch K., Payer S. E., Ertl C., Hofer G., Keller W., Braeuer S., Goessler W., Glueck S. M. and Himo F., Reaction mechanism and substrate specificity of iso-orotate decarboxylase: A combined theoretical and experimental study. *Front. Chem.*, **6** (2018), 608.

[27] Chen F., Zhao Y., Zhang C., Wang W., Gao J., Li Q., Qin H., Dai Y., Liu W. and Liu F., et al., A combined computational-experimental study on the substrate binding and reaction mechanism of salicylic acid decarboxylase. *Catalysts*, **12** (12) (2022), 1577.

[28] Prejanò M., Škerlová J., Stenmark P. and Himo F., Reaction mechanism of human PAICS elucidated by quantum chemical calculations. *J. Am. Chem. Soc.*, **144** (31) (2022), 14258-14268.